CELT TUBE STRUCTURE
FINAL CONCEPTUAL DESIGN

by

Stefan J. Medwadowski, Ph.D.

December 2001

SUMMARY

Described in this Report is the final conceptual design for the structure of the tube of CELT. Included are the physical description of the structure and its performance characteristics. In companion reports we present the final conceptual design of the yoke and the final conceptual design for the tube supports of the yoke.

The Report is accompanied by an electronic text, and by the model and solution files.

INTRODUCTION

The essence of an optical telescope is a system consisting of mirrors and instruments. The mirrors collect, redirect and focus the light; the instruments are used to study the properties of the light and to examine the image.

The primary role of the structure of the telescope is to support the mirrors and the instruments in the same relative position at all pointing directions. To allow for pointing, the structure of CELT consists of two parts: the tube, and the yoke. The tube supports the mirrors — primary, secondary and tertiary — and it rotates about the elevation axis. The yoke supports the tube as well as the instruments, which are located on the Nasmyth platforms. The yoke rotates in azimuth, and is supported by four bearings on a pier, and on a pintel in the center.

Described in this Report is the structure of the tube, at the level appropriate to the conceptual design phase. The structure of the yoke, and the performance of the tube-yoke assembly are described in separate reports.

DESCRIPTION OF THE STRUCTURE

The tube of CELT is in reality a single, rather stiff unit. However, its geometry is easiest described if we distinguish several component parts, as follows.

- Upper tube which supports the secondary socket and the secondary mirrors,
- Lower tube (or mirror cell) which supports the primary and tertiary mirrors,
- Two elevation journals attached to the base of the lower tube and which rest on the supports attached to the yoke.

Some of the overall dimensions of the tube are as follows.

- Distance from the primary vertex to the elevation axis: 3.50 m
- Distance from the primary vertex to the 4 m secondary: 39.40 m

- Outside radius of the primary (in x-y plane): 15.92 m
- Plan distance center-to-center of elevation journals: 22.65 m
- Radius of the arc of the elevation journals: 17.38 m
- Total height of the tube: 58 m

The first two dimensions are firm; the others are approximate.

A side view of the tube is shown in Figure 1.

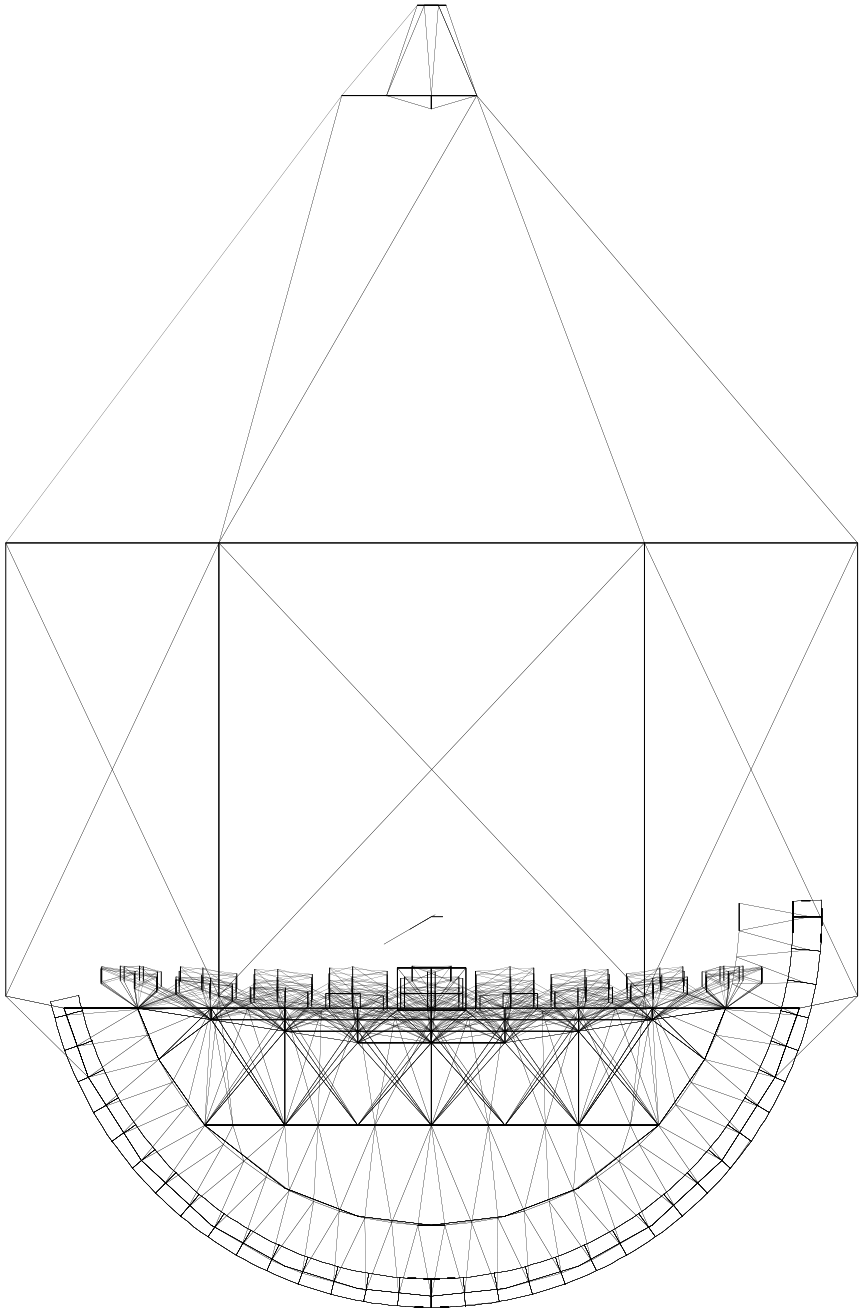

Figure 1 — Side view of the tube

Upper tube

Starting from the top, the upper tube consists of the following elements.

- Secondary socket, with the provision for support of a 4.00 m secondary, and a 1 m secondary for adaptive optics,
- The tripod, currently designed as continuum (non-latticed) elements with a square, 18 x18 tubular cross-section,
- A system of V-shaped braces - tension elements - (total 6), 1.5 x 6 , oriented in a vertical plane so as to reduce the light obstruction area; these elements are prestressed so that they are always in tension,
- A framed cylinder, hexagonal in plan, and located entirely outside the cylinder of incoming light, and connected to the mirror cell (lower tube) below. The frame consists of 6 verticals, a hexagonal ring, and 12 diagonals, all 18 x 18 tubes.

The geometry of the upper tube is shown in Figure 2a and 2b.

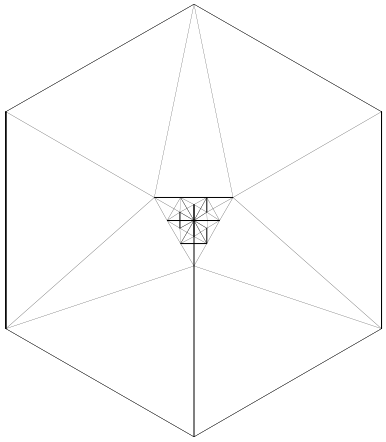

Figure 2a — Upper tube — Plan

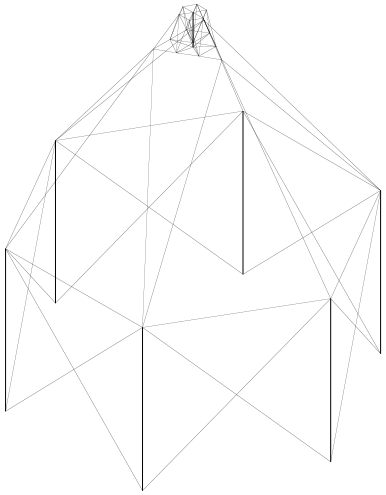

Figure 2b — Upper tube — Isometric view

Mirror cell (Lower tube)

The structure of the mirror cell is geometrically quite complex. It is a space frame with thousands of elements arranged in many layers. Figure 3 shows the side view of the mirror cell. It is similar to that shown in Figure 1, but several of the top layers have been shown exploded to illustrate more clearly their relative position. The exploded layers, from the top, are the tertiary tower, primary mirror, the cluster structures, the top layer of the mirror cell, and the layers of the diagonals, which connect the top layer to the layers below. Also not shown in Figure 3 are the elements located in the plane of the journals.

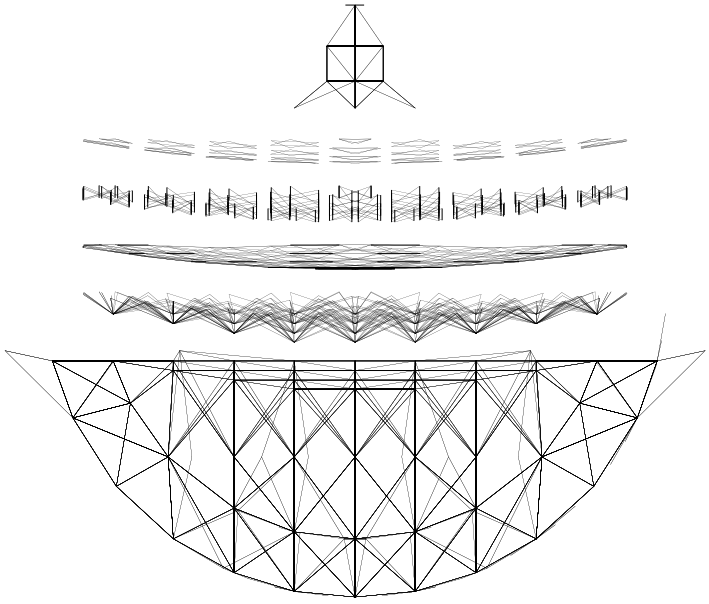

Figure 3 — Side view of the mirror cell, with some of the top layers exploded , and elements in the plane of the journals not shown

A plan of the computer model of the primary is shown in Figure 4. In this drawing, each triangle represents a cluster of segments (typically 19). The nodes of each triangle are located on a spherical surface of 90 m radius. The sides of the triangles are modeled as structural elements

of appropriate strength and stiffness; their weight density is such that, together, they correspond to the weight of the primary and its immediate support system.

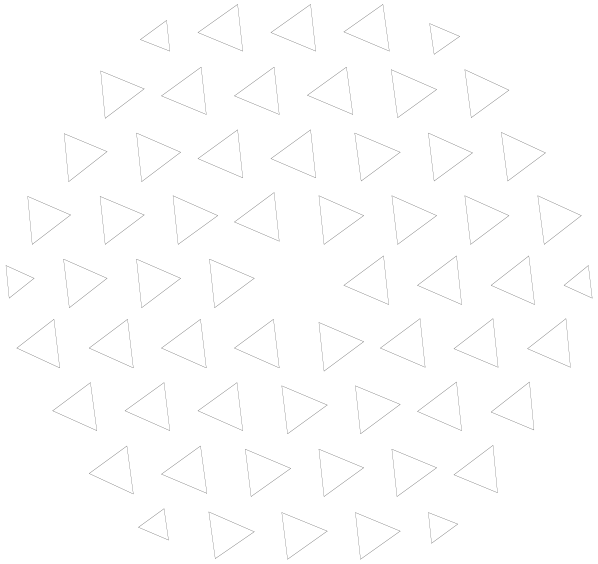

Figure 4 — Computer model representation of the primary mirror

The structure of the portion of the mirror cell below the exploded layers is shown in plan in Figure 5, and in side view in Figure 6. In the interior part, between the two journals, we have a nearly flat top layer and a flat intermediate layer, as well as two layers which are placed on circular cylindrical surfaces with centers on the elevation axis. In each case, the layers are based on a regular, triangular grid. These four layers are connected by three layers of diagonals, and five flat surfaces of elements parallel to the x-z plane. The total space frame is rather sparse. Additional groups of elements are provided to connect the upper tube to the mirror cell.

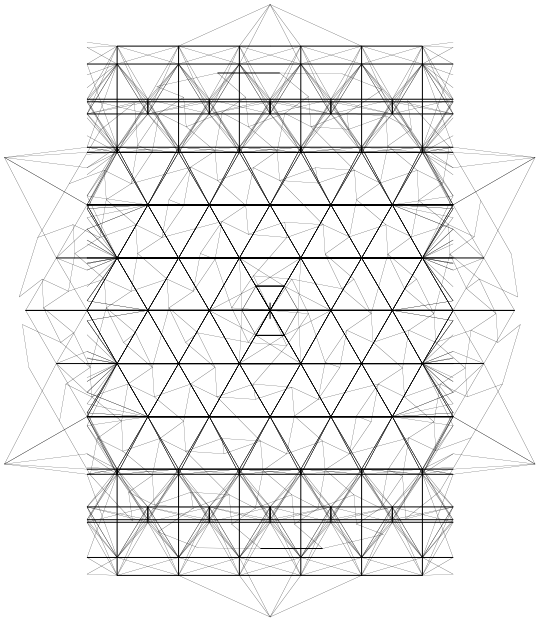

Figure 5 — Lower tube — Plan view — Several element layers removed for clarity

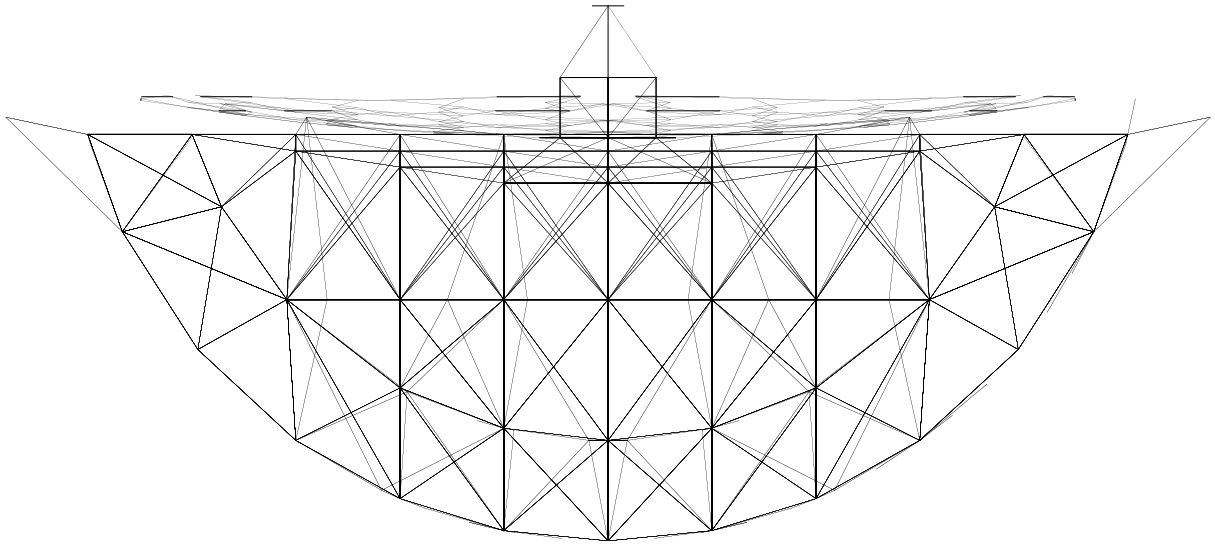

Figure 6 — Mirror cell — Side view — Primary and journals not shown for clarity

Finally, at each side of the mirror cell, in the plane of the elevation journals, there is a group of elements which, together with the journals, transfer all loads to the supports located on the yoke. These are shown in Figure 7.

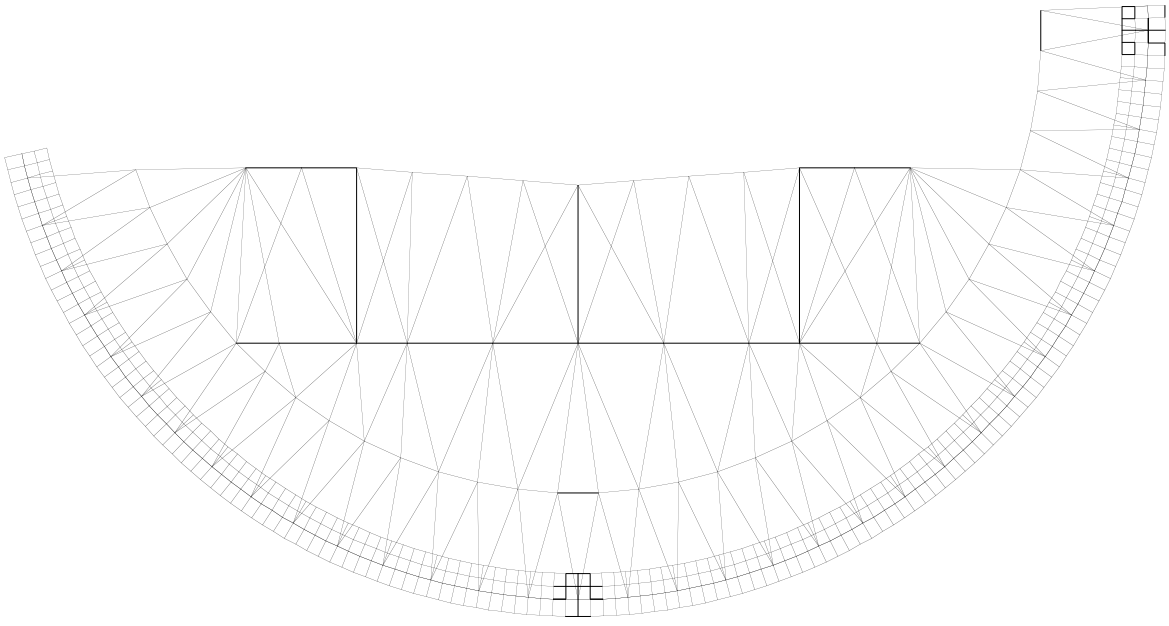

Figure 7 — Journal, and the elements in the plane if the journal — Side view

The support system is as follows. Each elevation journal is supported at six points. At three of these, the support acts only in the direction of a normal to the bearing surface of the journal. They restrain translations in the y- and z- directions; we assume that the weight of the tube is sufficiently great to prevent uplift. We note that this system is statically indeterminate. At two additional points, on each journal, a support is provided that is tangent to the arc of the journal, thus restraining rotation of the tube about the elevation axis. Finally, two supports on each journal restrain translation parallel to the elevation axis. Installation of these supports at both journals provides restraint against rotation about the y- and z- axes — thus all six degrees of freedom of motion are appropriately restrained. The support system is shown in Figure 8.

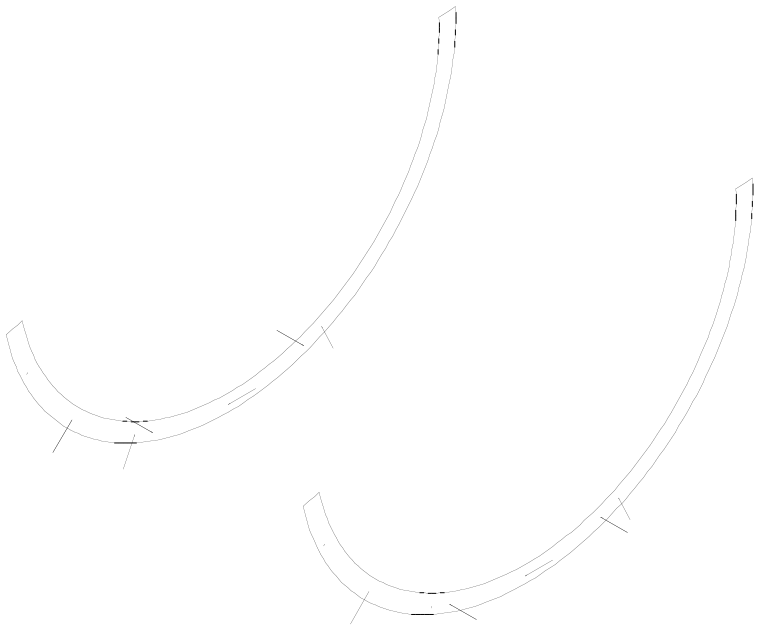

Figure 8 — A schematic representation of the tube support system

PERFORMANCE CHARACTERISTICS

We performed an analysis of the tube as an independent unit, supported not by the yoke but by a rigid medium. We considered several static loads and wind loads as described below, and also the dynamic characteristics. These analyses were performed for the tube pointing to 0^o, 30^o, 50^o and 65^o. To simplify the process of comparison of results we rotated not the tube itself, but rather the system of tube supports.

Because of the limitations of the application software, we used throughout the following system of units:

- Length: inch
- Force: kip (1 kip = 1000 pounds)
- Stress: ksi (kips per square inch)

The results of computer analyses are recorded in the sections that follow. The computer model was based on the geometry as described above. All elements were assumed steel, with cross-sectional properties adequate from the point of view of strength and stability. However, only limited optimization was attempted.

Weight, c.g., and moments of inertia

Weight of the tube: 1582.9 kips

Note: Included in this total is the weight of the mirrors and their supports (approx. 346 kips).

Center of gravity (to zenith): {0.069 , -0.0212 , 0.0937 }

Note: The slight imbalance is acceptable at this stage of design.

Mass moments of inertia (kips (sec^2/in) in^2)

Tube to zenith:

I_x = 1.5602E+06; I_y = 1.6047E+06; I_z = 1.1255E+06

Tube to 65^o:

I_x = 1.6602E+06; I_y = 1.6047R+06; I_z = 1.5008E+06

Gravity response

In analyzing the static response of the structure, we considered the following three load cases.

1. A combination of the gravity loads (the self-weight, and the superimposed loads) and prestressing,
2. Prestressing loads only,
3. Gravity loads only.

Support reactions

In the following, we report the magnitude of the reaction supports, the displacements at the secondary and the tertiary, and the displacements of the primary.

TABLE 1 — SUPPORT REACTIONSS UNDER GRAVITY AND PRESTRESSS LOADS

Pointing direction	*Reaction forces (kips)*				
	R_1	R_2	R_3	$\|R_4\|$	$\|R_5\|$
00^o	-154	-247	-505	<1	<99
30^o	-44	-382	-457	<2	<53
50^o	94	-553	-394	<3	<42
65^o	409	-938	-254	<2	<32

The meaning of the symbols R is as defined in a preceding section. Negative sign denotes compression, that is the tube pressing down on thee support. It is seen that the absolute value of R_4 is nearly zero, as it should be, since the tube is very nearly balanced. The absolute value of R_5 is relatively small, showing that the structure of the tube is fairly compliant. Finally, we note that the values of reactions R_1, R_2 and R_3 vary with the orientation of the tube. This is so, because the system of supports is not statically determinate, and the stiffness of the structure varies with the pointing orientation. We note also that the value of R_1 changes from negative to positive (from compression to tension) as the tube rotates toward 65^o.

In the analytical model the reactions are represented as concentrated forces. It is, therefore, of interest to examine the stress concentrations in the elements pf elevation journal. Figure 9 shows the minimum principal stresses in the web of the journal in the vicinity of reaction R_3 for the case of the tube pointing to zenith. The largest stress (in absolute value) is quite small, less than 9 ksi.

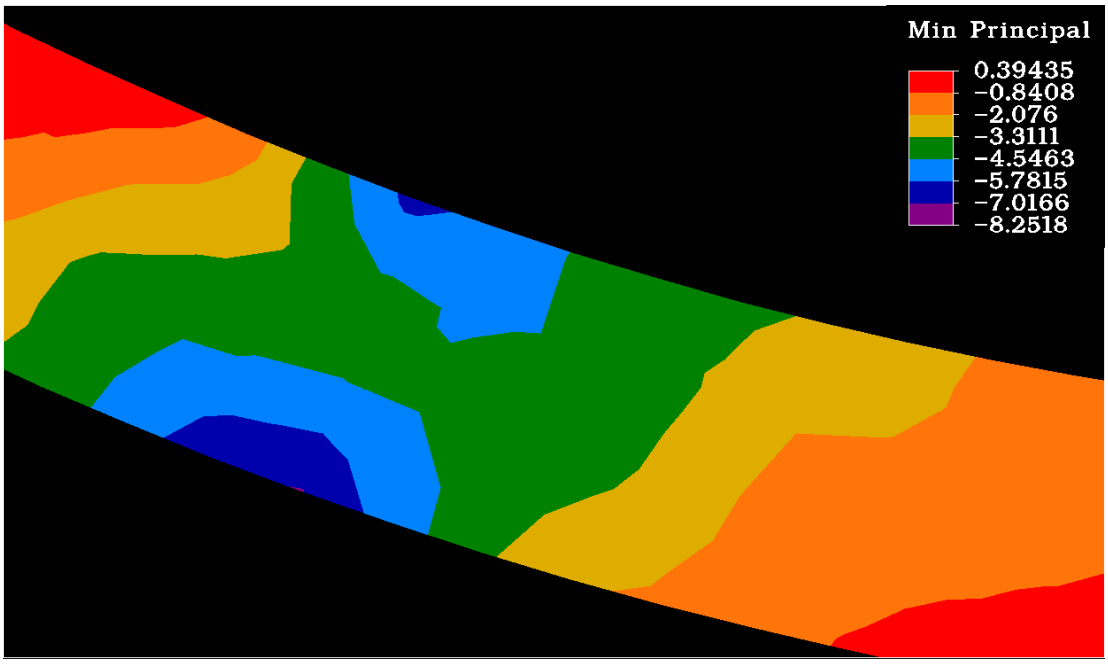

Figure 9 — Tube to zenith — Minimum principal journal stresses near reaction $\underline{R}$

Displacements of the secondary and tertiary

In TABLE 2 we report the displacements at the center of the 4 m secondary (node no. 3606), and the center if the tertiary (node no. 3532 or 3530, as noted), for the four different pointing directions of the tube.

TABLE 2 — SECONDARY AND TERTIARY DISPLACEMENTS UNDER GRAVITY AND PRESTRESS LOADS

Pointi direct	Node locat	Translations (inches)			Rotations (degrees)		
		Along x	Along y	Along z	About x	About y	About z
00°	3606	5.0893E-03	-9.2806E-01	-3.9413E+00	2.8558E-02	9.9376E-05	7.3197E-05
	3532	6.0927E-04	-1.4122E-01	-1.3218E-01	1.7880E-02	-1.1496E-04	1.4206E-05
30°	3606	2.4814E-03	-7.9232E-02	-3.8803E+00	3.8339E-02	-3.2734E-05	3.3926E-05
	3532	5.1277E-04	1.6813E-02	-1.1843E-01	2.0102E-03	-1.3236E-04	5.5582E-05
50°	3606	5.4802E-03	8.0539E-01	-3.7110E+00	2.9620E-02	1.8343E-05	-3.4250E-05
	3532	1.9055E-03	2.1794E-01	-7.8641E-03	-1.7955E-02	-7.6438E-05	1.0680E-04
65°	3606	1.7708E-03	2.3431E+00	-3.3477E+00	-6.3061E-03	-3.9935E-05	4.8532E-05
	3530	1.6519E-04	6.4065E-01	2.9077E-01	-6.0295E-02	-1.2467E-04	2.5643E-04

Displacements of the primary mirror segment clusters

As noted previously, the primary mirror is modeled as a collection of 60 clusters, each represented as a triangle with nodes at the surface of a sphere with the radius of 90 m. In the course of our analyses we obtained six components of displacement for each of the 180 nodes, for each of the four pointing directions. This information is supplied on an electronic medium, in the form of spreadsheets, well suited to additional manipulation. Here, we report only the average, the maximum and the minimum displacements of the 180 nodes.

TABLE 3 — DISPLACEMENTS OF THE PRIMARY CLUSTERS UNDER GRAVITY AND PRESTRESS LOADS

Pointi direct	Node locat:		Translations (inches)			Rotations (degrees)		
			Along	Along	Along z	About x	About y	About z
00°	*Average*	-8.4658E-04	-1.1302E-01	-1.1322E-01	1.6617E-02	-1.8411E-03	-1.3862E-03
	MAX	1.1361E-01	-3.3364E-02	1.0963E-01	7.2481E-02	1.0013E-01	2.7907E-02
	MIN	-1.1930E-01	-2.0660E-01	-4.2987E-01	-3.5449E-02	-8.4541E-02	-2.4640E-02
30°	*Average*	7.8686E-04	-4.1629E-03	-9.5331E-02	7.7722E-03	-6.3038E-04	-4.2611E-04
	MAX	1.1420E-01	6.8294E-02	5.4928E-02	5.8974E-02	1.0045E-01	2.5803E-02
	MIN	-1.1166E-01	-7.2257E-02	-3.3063E-01	-4.1221E-02	-8.3494E-02	-2.7054E-02
50°	*Average*	2.0460E-03	1.4904E-01	1.4151E-02	-8.4483E-03	-4.7427E-04	1.0051E-03
	MAX	1.1472E-01	2.1213E-01	2.0413E-01	4.9352E-02	9.7506E-02	2.7164E-02
	MIN	-1.1043E-01	9.9875E-02	-1.3726E-01	-5.5187E-02	-8.6875E-02	-2.5901E-02
65°	*Average*	0.000844826	0.484022	0.308713586	-0.04977608	-5.48633E-05	0.002287182
	MAX	1.1579E-01	5.6099E-01	7.7137E-01	1.2966E-02	9.7470E-02	3.1191E-02
	MIN	-1.1352E-01	4.1891E-01	-1.5597E-01	-9.3782E-02	-8.9929E-02	-2.7612E-02

Wind deflections

The effects of wind action at the secondary were allowed for by using concentrated load at the top successively in the direction of x-, y-, and z-axis. The magnitude of the load in each case was 1 kip. This approach, although approximate, yields some idea of the response of the structure to wind. The results are given in TABLE 3.

TABLE 3 — SECONDARY AND TERTIARY MIRRORS DISPLACEMENTS UNDER WIND LOADS AT THE TOP

Pointir directi	Node location	Translations (inches) Along x	Along y	Along z	Rotations (degrees) About x	About y	About z
00°	Secondar #3532	6.2058E-(	1.4569E-(	-5.0987E-	-3.2365E-	1.1749E-(	7.4914E-(
		-1.3180E-	6.2918E-(	-2.9841E-	-6.4882E-	6.4020E-(	-3.7102E-
		-8.1953E-	-2.0777E-	2.9819E-(	8.6390E-(	1.4643E-(	2.5632E-(
	Tertiary #3606	6.0315E-(	-3.7969E-	-2.0701E-	6.4253E-(	3.3626E-(	4.9997E-(
		3.2697E-	6.7550E-(	-5.8939E-	-3.6894E-	-2.2846E-	-1.4180E-
		-2.2286E-	-6.7509E-	9.5207E-(	-2.9689E-	3.9676E-(	1.1659E-(
30°	Secondar #3532	6.7002E-(	5.0038E-(	8.2922E-(	-5.6023E-	1.5273E-(	2.2388E-(
		-2.6420E-	7.1378E-(	1.6512E-(	-7.6943E-	2.6745E-(	2.2200E-(
		8.6400E-(	7.2755E-(	4.8935E-(	-8.5124E-	1.0500E-(	2.2404E-(
	Tertiary #3606	6.2257E-(	5.2851E-(	4.4127E-(	-4.3494E-	3.2835E-(	-1.0611E-
		7.2378E-(	7.2109E-(	2.9975E-(	-3.8349E-	-1.8718E-	-2.4470E-
		4.1396E-(	2.6240E-(	9.8372E-(	-1.8718E-	8.4580E-(	4.9066E-(
50°	Secondar #3532	7.0702E-(	4.7700E-(	-1.1582E-	-4.8382E-	2.3017E-(	5.8411E-(
		-5.6336E-	1.1067E-(	4.6287E-(	-1.2473E-	2.9367E-(	4.6369E-(
		5.2397E-(	1.4560E-(	9.6965E-(	-1.7961E-	6.8846E-(	3.0843E-(
	Tertiary #3606	6.3374E-(	2.2806E-(	2.5220E-(	-5.0357E-	3.1711E-(	5.1025E-(
		6.3374E-(	2.2806E-(	2.5220E-(	-5.0357E-	3.1711E-(	5.1025E-(
		2.4208E-(	5.7604E-(	1.0406E-(	-2.1870E-	3.0083E-(	7.4626E-(
Pointir directi	Node location	Translations (inches) Along x	Along y	Along z	Rotations (degrees) About x	About y	About z
65°	Secondar #3530	8.9094E-(	6.8488E-(	-2.0942E-	-9.1396E-	4.0034E-(	1.0695E-(
		-4.7969E-	2.1913E-(	1.3485E-(	-2.3625E-	4.0831E-(	6.9403E-(
		2.0235E-(	3.7567E-(	2.6768E-(	-4.1507E-	1.3952E-(	3.3726E-(

	Tertiary #3606	6.7235E-0 6.6585E- 2.1282E-0	-8.5142E- 1.2564E-0 1.3909E-0	9.7207E-0 1.5362E-0 1.2072E-0	-1.2937E- -5.4668E- -4.6168E-	3.1109E-0 -4.6121E- -3.8013E-	1.1464E-0 1.5352E-0 9.2734E-0

The largest (in absolute value) component of translation of the secondary (node #3606) occurs with the tube pointing to 65°, when the wind acts in the direction if the y-axis.

Natural frequencies

The three lowest frequencies for the four pointing directions are shown in TABLE 4.

TABLE 4 - NATURAL FREQUENCIES OF THE TUBE

Pointing direction	***Mode no.***	***Frequency (Hz)***	***Mode shape (principal component only)***
00°	*1*	2.61	Rocking motion in the y-z plane
	2	2.69	Rocking motion in the x-z plane
	3	5.41	2nd mode in the x-z plane
30°	*1*	2.51	Rocking motion in the y-z plane
	2	2.64	Rocking motion in the x-z plane
	3	4.58	Torsion about the z-axis
50°	*1*	2.21	Rocking motion in the y-z plane
	2	2.59	Rocking motion in the x-z plane
	3	4.14	Torsion about the z-axis
65o	*1*	1.74	Rocking motion in the y-z plane
	2	2.42	Rocking motion in the x-z plane
	3	3.39	Torsion about the z-axis

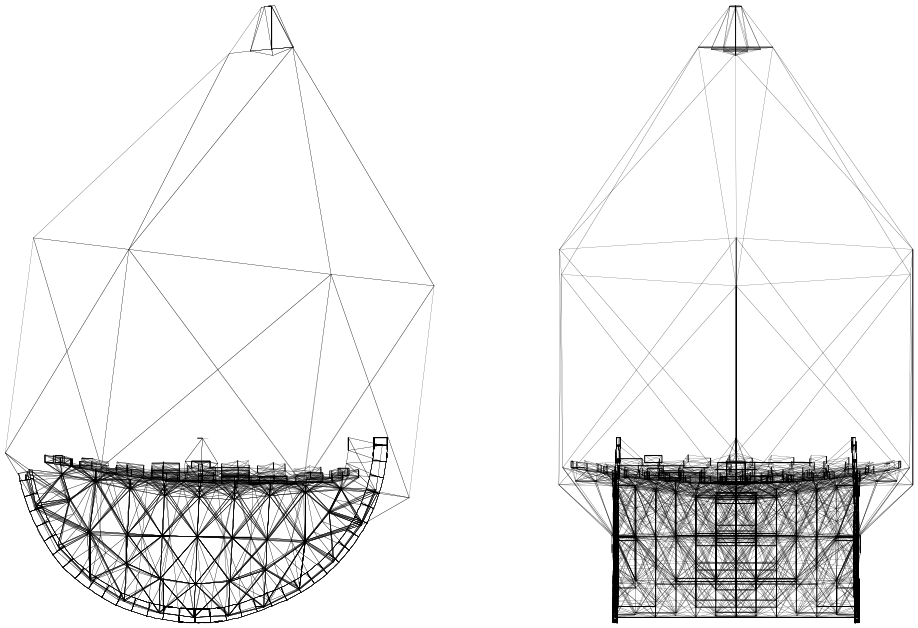

Figure 10 — Tube to zenith, 1st mode, f=2.61 Hz — Side and front elevations

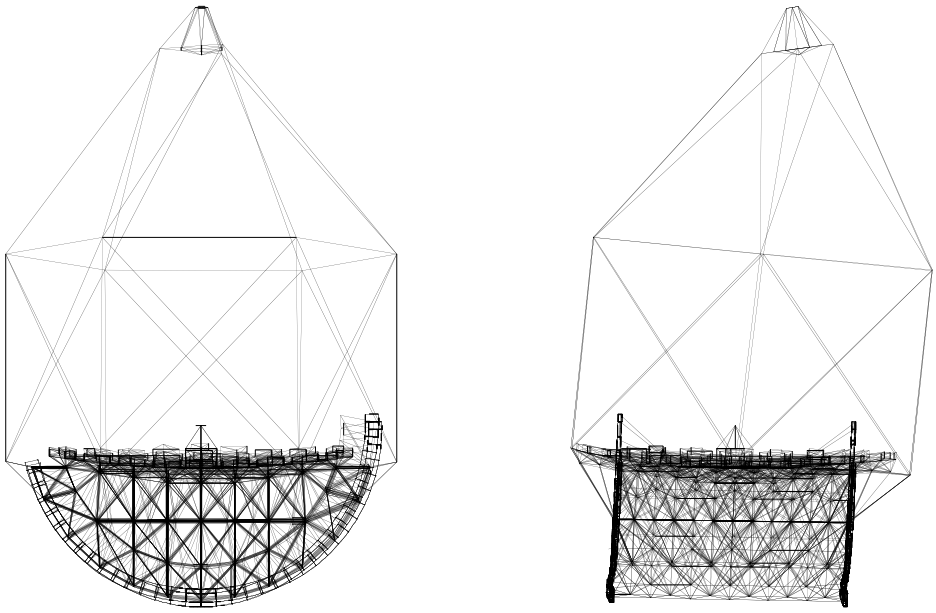

Figure 11 — Tube to zenith, 2nd mode, f=2.69 Hz — Side and front elevations

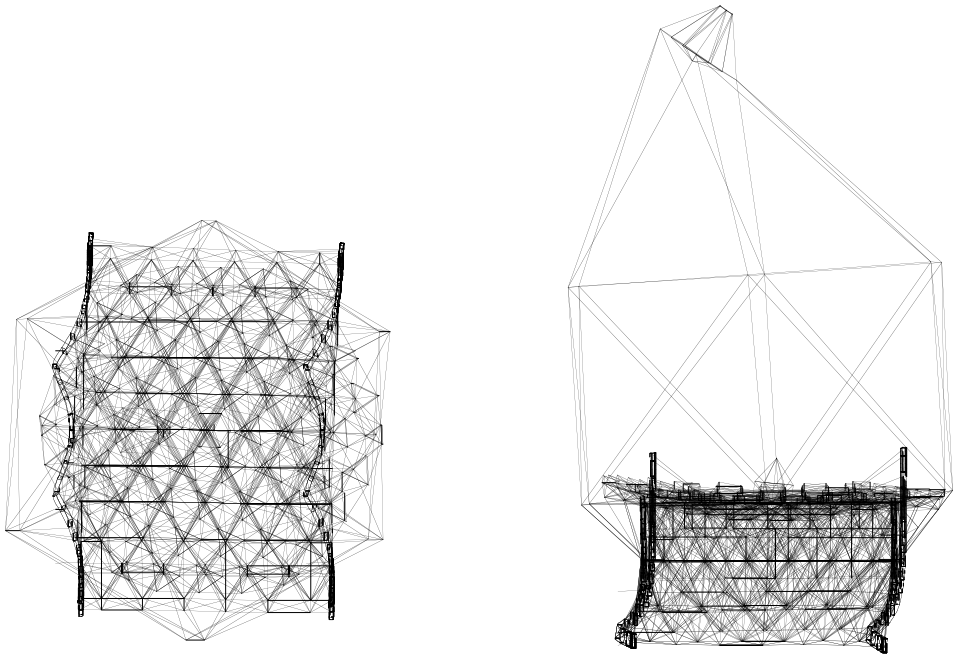

Figure 12 — Tube to zenith, 3rd mode, f=5.41 Hz — Plan and front elevation

In all cases, the third mode shape is a combination of rotation of the tube about the optical axis, and the second mode associated with the motion in the x-z plane. The latter effect grows in importance as the inclination angle of the tube increases. It is seen that the sequence of mode shapes is very nearly independent of the pointing direction. When the tube points to the zenith, the two lowest frequencies are very nearly the same. The greater the inclination of the tube, the smaller is the first frequency. However, the loss of dynamic stiffness is relatively small until the angle is greater than approx. 50 degrees. At that point, the tube is supported on the cantilevered (and hence least stiff) parts of the elevation journals.

DISCUSSION

We wish to offer the following comments on the structure as presented above.

- The weight of the tube, at approx. 1580 kips (720 tons), is somewhat less than the weight of the latticed tetrapod tube we previously reported on[1], and it is relatively small.
- The response of the tube to the gravity+prestress loads is acceptable; the response to wind at the secondary has to be studied in detail before definitive conclusions can be drawn.
- The upper tube — the braced tripod on a hexagon — is very stiff. However, the tube as a whole has the lowest frequency of only 2.61 Hz. when pointing to zenith, and even less than that, only 1.74 Hz., when pointing to 65^{o}. We conclude that the lower tube should be redesigned to increase the dynamic stiffness. Some improvement can be obtained by optimizing the distribution of mass to the elements of the tube. However, we are of the opinion that principal effort should be exerted in the direction of re-examining the geometry and the topology of the structure.
- If at all possible, the additional supports at —45o angle to azimuth should nit be used.

We believe that it is reasonable to conclude that the tube structure presented above is a suitable candidate solution, and a good starting point for further design work. However, as noted

[1] Medwadowski, S. J., The structure of the tube of the CELT telescope, June 2001 (TN6).

above, the topology and the geometry of the lower tube need to be re-examined to improve the dynamic stiffness of the system.

ACKNOWLEGMENTS

The many enlightening discussions with Jerry Nelson have been much appreciated. We acknowledge the input and assistance of Peter Wrona. The help and patience of Betty Medwadowski have been beyond measure.

ATTACHMENTS

Attached to this Report is a number of files on electronic media. These files are listed below.

1. This Report, in file CELT TN #10
2. Spreadsheet files

   There are four files: 00 XYZ-UVW, 30 XYZ-UVW, 50 XYZ-UVW, and 65 XYZ-UVW. Each of these files is organized as follows.

   Sheet 1: col. A and G: node number

   Cols. B-D: x-, y- and z-coordinates of the node

   Cols. H-M: six components of displacement of the node

   Sheet 2: cols. A and G: node number

   Cols. B-D: x-, y- and z-coordinates of the node

   Cols. H-M: six components of displacement of the node

   Col. Q: Cluster number (1 to 60)

   Cols. R and S: x- and y-coordinates of the center of gravity of cluster; the three nodes of a given cluster are within a circle of 1.5 m radius of the center of gravity
3. Drawing files

   C AALL

   T ALL to Z

   T ALL to 30

   T ALL to 65

   Y+T-FRONT

   Y+T-SIDE to 30

   Y ALL
4. Analysis files, in 4 folders

   TUBE to 00, TUBE to 30, TUBE to 50, and TUBE to 65.

   Each of these folders contains numerous problem definition and solution files named GB-TUBE to ??.*, where the symbol ?? denotes (00, 30, 50, or 65).